ISSN (e) 2520-7393
ISSN (p) 2521-5027
www.estirj.com

Variable On-Time Control Scheme to Improve the Efficiency for AC-DC Integrated Buck /Boost Converter

Salman Ayaz Memon[1], A. Hakeem Memon[1], Zubair Ahmed Memon[1], Munwar Ayaz Memon[2]

[1]*Department of Electrical Engineering, Mehran University of Engineering and Technology, Jamshoro, 76062, Sindh Pakistan*
[2]*Department of Electrical Engineering, Quaid-e-Awam University of Engineering Science and Technology, Nawabshah, Sindh Pakistan*

Abstract: The critical conduction mode buck converter is a good topology due to it providing features such as protection against short circuits, low output-voltage at high input-voltage, low inrush-current, low voltage gain ratio gives small output-voltage ripple. However due to dead zone, its input power factor is low. The power factor can be made higher by introducing boost converter to work with buck converter at the time of dead zone. Though, when the on time of the switch is constant due to operation in traditional control technique (TCT), its efficiency is low. Due to the large peak and rms values of the inductor current, there are significant conduction and switching losses, which are the main cause of the low efficiency. This publication presents a variable on-time control strategy that reduces peak current values and thus improves performance. The proposed study focuses on the critical conduction mode integrated buck-boost (CRMIBB) converter. The main contribution of the paper is that it requires only feed-forward circuits in buck switch as compared to other research work to improve the efficiency of the CRM buck converter. Using SABER SIMULATOR, a comparison of the proposed control technique (PCT) and the traditional control technique (TCT) is achieved to confirm the efficiency of the PCT. The efficiency of the (CRMIBB) converter is found to be enhanced by (PCT) in comparison to TCT.

Keywords: *Critical conduction mode integrated buck-boost (CRMIBB); traditional control technique (TCT); proposed control technique (PCT); Saber Simulator*

1. Introduction

Due to the growing demand for electronic devices, which necessitates the conversion of AC to DC, the non-linear components (such as diode & thyristor) generate the harmonic content in electronic equipment connected to AC power system must be within a certain range in order to comply with regulatory standards. This criterion is achieved by modifying the input phase current such that it has a sinusoidal shape and is in phase with the input phase voltages using active power factor improvement (PFI) circuits.

Non-linear loads working simultaneously create a major harmonic distortion issue in the electrical distribution system, which has negative effects on the voltage distortion, power quality, power factor, and efficiency [1]. Power factor improvement divided into passive & active different categories. An active power factor improvement converter (PFIC) can obtain a high PF when compared to a passive PFIC [2-14]. PFICs are commonly utilized in AC-DC power converters to eliminate harmonic distortion & achieve unity power factor to meet standards such as IEEE 519 and IEC61000-3-2 [15-16]. Buck Power Factor Improvement Converters (BPFICs) are considerably superior topologies than PFICs because they provide benefits including lower inrush current, lower voltage gain ratio, lower output voltage ripple, protection against short circuits, and single active switch operation. However, the dead zone in the (BPFIC) input current has led to low power factor (PF) and other power quality problems. Various researchers have suggested several control approaches to improve the efficiency of BPFIC [17-30]. This research paper implements the proposed control technique (PCT), in order to decrease conduction and switching losses caused by the peak and average values of inductor current in a critical conduction mode integrated buck-boost converter (CRMIBB).The main contribution of the paper is that it requires only feed-forward circuits in buck switch as compared to other research work to improve the efficiency of the CRM buck converter

There are six portions in this paper. The first portion provides a thorough review of the (CRMIBB) converter using conventional control methodology. In second part (PCT) is implemented, to increase the effectiveness of the (CRMIBB) converter. Conduction and switching losses are analyzed in the third portion of the paper. The simulated verification in the fourth part demonstrates the PCT's efficiency. The final part discusses the result.

2. Traditional Control Technique for Critical Conduction mode Integrated BUCK/BOOST Converter

The basic circuit of the converter (CRMIBB) is shown in Figure 1. It is a buck converter using a normal inductor in series with a boost converter. It operates in buck mode with the boost switch open when the instantaneous input line voltage is greater than the boundary voltage; otherwise, it operates in boost mode with the buck switch closed. Compared to the output voltage, the boundary voltage is slightly higher. The converter uses CRM, and its operation can be analyzed in two cases.

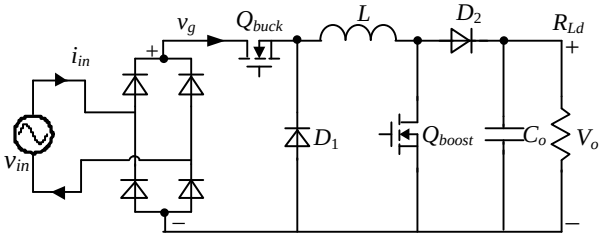

Figure.1. Block diagram of IBBC

Mathematically, the input and rectified input voltage are written as

$$v_{in}(\theta) = \sqrt{2}V_{rms}\sin\theta \tag{1}$$

$$v_g = \sqrt{2}V_{rms}|sin\,\theta| \tag{2}$$

Here, V_{rms} is the value of rms.

IBBC will operate in buck mode till input voltage exceeds the boundary voltage. Hence, Q_{buck} works when Q_{boost} turned off.

When the buck switch is turned on, the maximum inductor current and average value of input is expressed as

$$i_{L(pk1)}(\theta) = \frac{\sqrt{2}V_{rms}|sin\,\theta|-V_o}{L}t_{on} \quad (\theta_o \le \theta \le \pi - \theta_o) \tag{3}$$

Where $\theta_0 = \arcsin\dfrac{V_{boundary}}{\sqrt{2}V_{rms}}$

$$i_{(avg)buck}(\theta) = \left(\frac{(\sqrt{2}V_{rms}|sin\,\theta|-V_o)}{\sqrt{2}V_{rms}|sin\,\theta|}\right)\frac{t_{on}V_o}{2L} \tag{4}$$

The IBBC will work in boost mode till input voltage is less than the boundary voltage. Hence, Q_{boost} operates when Q_{buck} is turned off

When the boost switch is turned on, the maximum inductor current and average input current is expressed as

$$i_{L(pk2)}(\theta) = \frac{\sqrt{2}V_{rms}|\sin\theta|}{L}t_{on} \tag{5}$$

$$i_{boost(avg)}(\theta) = \frac{\sqrt{2}V_{rms}|\sin\theta|}{2L}t_{on} \tag{6}$$

According to the analysis, the (CRMIBB) converter with TCT has the following average input current.

$$i_{in(TCT)}(\theta) = \begin{cases} \dfrac{t_{on}\sqrt{2}V_{rms}|\sin\theta|}{2L} & (0 \le \theta < \theta_o \,\&\, \pi - \theta_o < \theta \le \pi) \\ \left(\dfrac{\sqrt{2}V_{rms}|\sin\theta| - V_o}{\sqrt{2}V_{rms}|\sin\theta|}\right)\dfrac{t_{on}V_o}{2L} & (\theta_o \le \theta \le \pi - \theta_o) \end{cases} \tag{7}$$

The input power of the IBBC is stated as follows from (1) and (6) respectively;

$$P_{in\_TCT} = \left[2\int_0^{\theta_o}\left(\sqrt{2}V_{rms}|\sin\theta|\right)^2 d\theta + \int_{\theta_o}^{\pi-\theta_o} V_o\left(\sqrt{2}V_{rms}|\sin\theta| - V_o\right)d\theta\right]\frac{t_{on}}{2\pi L} \tag{8}$$

Assuming IBBC efficiency is 100%, t_{on} may now be calculated.

$$t_{on} = \frac{2\pi P_o L}{\left[2\int_0^{\theta_o}\left(\sqrt{2}V_{rms}|\sin\theta|\right)^2 d\theta + \int_{\theta_o}^{\pi-\theta_o} V_o\left(\sqrt{2}V_{rms}|\sin\theta| - V_o\right)d\theta\right]}$$

3. Proposed Control Technique for Critical Conduction mode Integrated BUCK/BOOST Converter

The input current can be written as follow for high efficiency and power balance

$$i_{in}(\theta) = \frac{\sqrt{2}P_o|\sin\theta|}{V_{rms}} \tag{9}$$

We can obtain the desired on time of buck switch by combining (4) and (9).

$$t_{on\_b} = k_{on}\frac{(V_m\sin\theta)^2}{V_o(V_m\sin\theta - V_o)} \tag{10}$$

For the boost switch, there is no need of any variation of time. So no need of feed forward circuits.

According to the proposed control strategy, the input power is

$$P_{in\_PCT} = \frac{1}{\pi}\int_0^{\pi}(v_{in}.i_{in})d\theta = \frac{k_{on}V_m^2}{4L} \tag{11}$$

By assuming 100% efficiency, the value of k_{on} is obtained.

$$k_{on} = \frac{4P_oL}{V_m^2} \tag{12}$$

4. Analysis of Power Loss

The rms current of switch Q_b and $Q_{b/b}$ during the on-time period, which may be obtained as

$$I_{rms(Qb/b\_on)} = \frac{\sqrt{2\int_0^{\theta_o} i_{L(pk2)}^2(\theta)Dd\theta}}{3\pi} \quad (13\ (a))$$

$$I_{rms(Qb\_on)} = \sqrt{\frac{\int_{\theta_o}^{\pi-\theta_o} i_{L(pk1)}^2(\theta)Dd\theta}{3\pi}} \quad (13(b))$$

The off-time period's rms current may be calculated as

$$I_{(Qb/b\_off)rms} = \frac{\sqrt{2\int_0^{\theta_o} i_{(pk2)L}^2(\theta)(1-D)d\theta}}{3\pi} \quad (13(c))$$

$$I_{(Qb\_off)rms} = \sqrt{\frac{\int_{\theta_o}^{\pi-\theta_o} i_{(pk1)L}^2(\theta)(1-D)d\theta}{3\pi}} \quad (13(d))$$

Here

$$D = \begin{cases} \frac{V_o}{V_m \sin\theta} & Q_b Conducting \\ \frac{V_o}{V_o + V_m \sin\theta} & Q_{b/b} Conducting \end{cases} \quad (14)$$

As Q_b and $Q_{b/b}$ are turned on and turned off, current flow through inductor's windings, and its rms current is

$$I_{(TCT)rms} = \sqrt{I_{(Q_b\_on\_TCT)rms}^2 + I_{(Q_b\_off\_TCT)rms}^2 + I_{(Q_{b/b}\_on\_TCT)rms}^2 + I_{(Q_{b/b}\_off\_TCT)rms}^2} \quad (15\ (a))$$

$$I_{(PCT)rms} = \sqrt{I_{(Q_b\_on\_PCT)rms}^2 + I_{(Q_b\_off\_PCT)rms}^2 + I_{(Q_{b/b}\_on\_PCT)rms}^2 + I_{(Q_{b/b}\_off\_PCT)rms}^2} \quad (15(b))$$

4.1 Losses of the Bridge Rectifier

The formula below is used to calculate the loss of the bridge rectifiers.

$$P_{(TCT)bridge\_con} = 2V_{FD}I_{(TCT)avg\_in} \quad (16\ (a))$$

$$P_{(PCT)bridge\_con} = 2V_{FD}I_{(PCT)avg\_in} \quad (16(b))$$

The rectifier bridge KBL10 is adopted, and its forward voltage drop VFD is 0.89V. The suggested control strategy and the traditional input current are both specified as

$$I_{in_{avg(TCT)}} = \frac{1}{\pi}\left[\begin{array}{l} \int_0^{\theta_o} \frac{\frac{\pi P_o V_o V_m \sin\theta}{(V_o+V_m\sin\theta)}}{\int_0^{\theta_o}\frac{V_o(V_m\sin\theta)^2}{(V_o+V_m\sin\theta)}d\theta+\int_{\theta_o}^{\pi/2}V_o(V_m\sin\theta-V_o)d\theta} d\theta \\ + \int_{\theta_o}^{\pi-\theta_o} \frac{\frac{V_o}{2}\left(\frac{V_m\sin\theta-V_o}{V_m\sin\theta}\right)}{\int_0^{\theta_o}\frac{V_o(V_m\sin\theta)^2}{(V_o+V_m\sin\theta)}d\theta+\int_{\theta_o}^{\pi/2}V_o(V_m\sin\theta-V_o)d\theta} d\theta \end{array}\right] \quad (17\ (a))$$

$$I_{(PCT)avg\_in} = \frac{4P_o}{\pi V_m} \quad (17(b))$$

4.2 The Switches' Turn-On Losses

The losses from switch conduction may be obtained as

$$P_{(TCT)switch_{con}} = I_{(TCT\_on\_Q_b)rms}^2 R_{(on)DS\_Q_b} + I_{(TCT\_on\_Q_{b/b})rms}^2 R_{(on)DS\_Q_{b/b}} \quad (18\ (a))$$

$$P_{(PCT)switch_{con}} = I_{(PCT\_on\_Q_b)rms}^2 R_{(on)DS\_Q_b} + I_{(PCT\_on\_Q_{b/b})rms}^2 R_{(on)DS\_Q_{b/b}} \quad (18(b))$$

The value of 0.19 for $R_{DS(on)}$ for the switch 20N60C3 is taken from the datasheet.

4.3 The Switches' Turn-Off Losses

According to the traditional and suggested control strategy, the turn off loss of the buck & buck/boost switches may be calculated as

$$P_{(TCT)switches\_off} = \left[\begin{array}{l} 2\int_0^{\theta_o} \frac{i_{(TCT\_pk2)L}(V_m\sin\theta+V_o)}{2} t_{f1} f_{(TCT)s} d\theta \\ + \int_{\theta_o}^{\pi-\theta_o} \frac{i_{(TCT\_pk1)}(\theta)V_m\sin\theta}{2} t_{f2} f_{(TCT)s} d\theta \end{array}\right]\frac{1}{\pi} \quad (39(a))$$

$$P_{(PCT)switches_{off}} = \left[\begin{array}{l} 2\int_0^{\theta_o} \frac{i_{(PCT\_pk2)L}(V_m\sin\theta+V_o)}{2} t_{f1} f_{(PCT)s} d\theta \\ + \int_{\theta_o}^{\pi-\theta_o} \frac{i_{(PCT\_pk1)L}(\theta)V_m\sin\theta}{2} t_{f2} f_{(PCT)s} d\theta \end{array}\right]\frac{1}{\pi} \quad (19(b))$$

Based on the datasheet, the turn-off fall time for CMOS 20N60C is 12ns.

With both control strategies, the inductor current's peak-value is expressed.

$$i_{(TCT)pk} = \begin{cases} i_{(TCT\_pk2)L} = \frac{\pi P_o V_m \sin\theta}{\int_0^{\theta_o}\frac{V_o(V_m\sin\theta)^2}{(V_o+V_m\sin\theta)}d\theta + \int_{\theta_o}^{\pi/2}V_o(V_m\sin\theta-V_o)\,d\theta} \\ i_{(TCT\_pk1)} = \frac{\pi P_o(V_m\sin\theta-V_o)}{\int_0^{\theta_o}\frac{V_o(V_m\sin\theta)^2}{(V_o+V_m\sin\theta)}d\theta + \int_{\theta_o}^{\pi/2}V_o(V_m\sin\theta-V_o)\,d\theta} \end{cases} \quad (20(a))$$

$$i_{(PCT)pk} = \begin{cases} i_{(PCT\_pk2)L} = \frac{4P_o\sin\theta(V_o+V_m\sin\theta)}{V_m V_o} \\ i_{(PCT\_pk1)L} = \frac{4P_o\sin\theta^2}{V_o} \end{cases} \quad (20(b))$$

For both control schemes, the switching frequency may be determined as

$i_{(TCT)pk} =$

$$\begin{cases} i_{TCT\_pk2)L} = \dfrac{\pi P_o V_m \sin\theta}{\int_0^{\theta_o} \frac{V_o(V_m \sin\theta)^2}{(V_o+V_m \sin\theta)} d\theta + \int_{\theta_o}^{\pi/2} V_o(V_m \sin\theta - V_o)\, d\theta} \\ i_{(TCT\_pk1)} = \dfrac{\pi P_o(V_m \sin\theta - V_o)}{\int_0^{\theta_o} \frac{V_o(V_m \sin\theta)^2}{(V_o+V_m \sin\theta)} d\theta + \int_{\theta_o}^{\pi/2} V_o(V_m \sin\theta - V_o)\, d\theta} \end{cases}$$

(21(a))

$$i_{(PCT)pk} = \begin{cases} i_{(PCT\_pk2)L} = \frac{4P_o \sin\theta (V_o + V_m \sin\theta)}{V_m V_o} \\ i_{(PCT\_pk1)L} = \frac{4P_o \sin\theta^2}{V_o} \end{cases} \quad (21(b))$$

The switching frequency is calculated as

$$f_{(TCT)s} =$$

$$\begin{cases} \dfrac{V_o\left(\int_0^{\theta_o} \frac{V_o(V_m \sin\theta)^2}{V_o+V_m \sin\theta} d\theta + \int_{\theta_o}^{\pi/2} V_o(V_m \sin\theta - V_o)\, d\theta\right)}{\pi P_o L(V_o + V_m \sin\theta)} \\ \dfrac{V_o\left(\int_0^{\theta_o} \frac{V_o(V_m \sin\theta)^2}{V_o+V_m \sin\theta} d\theta + \int_{\theta_o}^{\pi/2} V_o(V_m \sin\theta - V_o)\, d\theta\right)}{\pi P_o L V_m \sin\theta} \end{cases}$$

(22(a))

$$f_{(PCT)s} = \begin{cases} \frac{V_m^2 V_o}{2P_o L(V_m \sin\theta + V_o)^2} \\ \frac{V_o^2(V_m \sin\theta - V_o)}{4P_o L V_m \sin^3\theta} \end{cases} \quad (22(b))$$

4.4 The Inductor's Copper Losses

The copper losses of the inductor with the proposed & conventional control schemes is expressed

$$P_{(TCT)copper} = I_{rms(TCT)}^2 R_{copper} \quad (23(a))$$

$$P_{(PCT)copper} = I_{rms(PCT)}^2 R_{copper} \quad (23(b))$$

The equivalent resistance of the copper wire is 0.1ohms.

4.5 The Core Losses of Inductor

The core losses of the inductor under the proposed & conventional control schemes is determined as

$$P_{core(TCT)} = \frac{10^3 V_e}{\pi}\left[\int_0^{\pi} C_m f_{(TCT)s}{}^x B_{(TCT)ac}{}^y (Ct_0 - Ct_1 T_a - Ct_2 T_a^2) d\theta\right] \quad (24(a))$$

$$B_{(TCT)ac} = \begin{cases} \frac{Li_{(TCT\_pk2)L}}{2NA_e} \\ \frac{Li_{(TCT\_pk1)L}}{2NA_e} \end{cases} \quad (24(b))$$

$$P_{(PCT)core} = \frac{10^3 V_e}{\pi}\left[\int_0^{\pi} C_m f_{(PCT)s}{}^x B_{(PCT)ac}{}^y (Ct_0 - Ct_1 T_a - Ct_2 T_a^2) d\theta\right] \quad (24(c))$$

$$B_{(PCT)ac} = \begin{cases} \frac{Li_{(PCT\_pk2)L}}{2NA_e} \\ \frac{Li_{(PCT\_pk1)L}}{2NA_e} \end{cases} \quad (24(d))$$

4.6 The Freewheeling Diode's Conduction Losses

The freewheeling diode's conduction loss is expressed as

$$P_{(TCT)con\_freewheelingdiode} = \frac{V_{FD_{fw}}}{\pi}\int_0^{\pi} \frac{i_{(TCT)pk}}{2}[1 - D] d\theta \quad (25(a))$$

$$P_{(PCT)con\_freewheelingdiode} = \frac{V_{FD_{fw}}}{\pi}\int_0^{\pi} \frac{i_{(PCT)pk}}{2}[1 - D] d\theta \quad (25(b))$$

The freewheeling diode MUR 1560 has a 0.67 forward voltage drop.

4.7 The Theoretical Efficiency

The following formula may be used to determine the theoretical effectiveness of both the conventional and proposed control schemes.

$$\eta_{TCT} = \frac{P_o}{\left[\begin{matrix} P_o + P_{TCT(con\_bridge)} + P_{TCT(con\_switches)} + P_{TCT(off\_switches)} \\ + P_{TCT(copper)} + P_{TCT(core)} + P_{TCT(con\_freewheelingdiode)} \end{matrix}\right]} \quad (26(a))$$

$$\eta_{PCT} = \frac{P_o}{\left[\begin{matrix} P_o + P_{PCT(con\_bridge)} + P_{PCT(con\_switches)} + P_{PCT(off\_switches)} \\ + P_{PCT(copper)} + P_{PCT(core)} + P_{PCT(con\_freewheelingdiode)} \end{matrix}\right]} \quad (26(b))$$

Figures 2-4 show the loss distribution at 90 VAC, 220 VAC, and theoretical efficiency, respectively, based on the analysis and converter parameters mentioned above. It is clear that the suggested control strategy increases efficiency while decreasing the converter's overall losses.

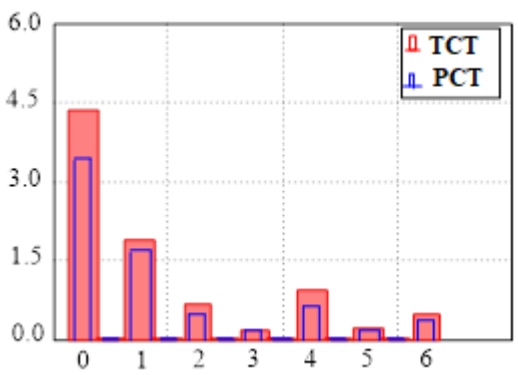

Figure.2. Loss Distribution at 90VAC

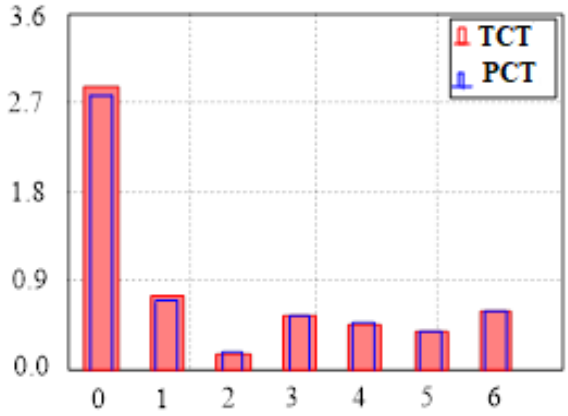

Figure.3. Loss Distribution at 220VAC

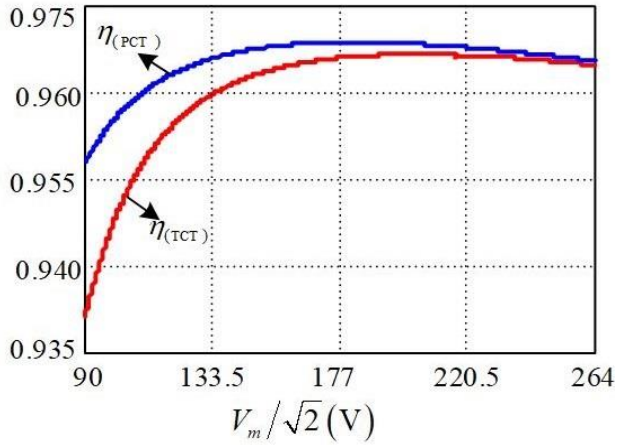

Figure.4. A universal input voltage efficiency

5. Simulation Verification

Simulations are used to confirm the suggested strategy's efficiency. The output voltage is 80V, while the input voltage ranges from 90 to 264 VAC. L6561 IC is used to ensure that the current is in CRM. The circuit's components have all been chosen as an ideas.

Figure 5 and 6 show simulated waveforms at 220 VAC input of v_{in} i_{in} and V_o of CRMIBB converter at 220 VAC input with the conventional and proposed control strategy, respectively. When compared to the traditional control strategy, it shows that with the suggested control strategy the input current is lower. Therefore, compared to TCT, the total conduction loss of variable on-time control technique (VOTC) is lower. The VOTC is same as PCT. In variable on-time control technique the constant on-time of the buck switch is made variable

According to the boundary voltage between the converter's switches in both types of control schemes, the gate drive signals for the converter's switches, through which the converter operates either in buck mode or buck/boost mode, are shown in Figure 7.

Figure 8 shows the PF comparison of CRMIBB converter between TCT and PCT. It can be observed that PF is improved a lot in case of PCT.

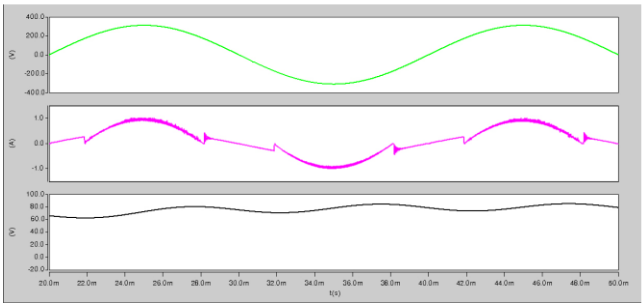

Figure.5. Shows traditional control with v_{in}, i_{in} and V_o

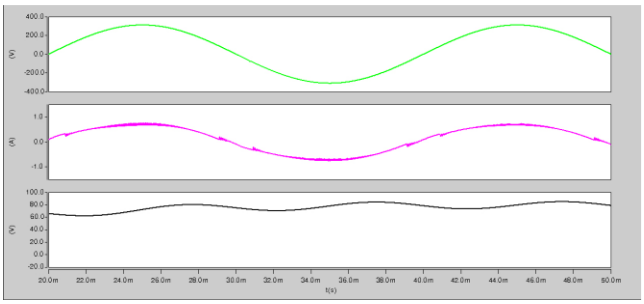

Figure.6. Shows proposed control with v_{in}, i_{in} and V_o

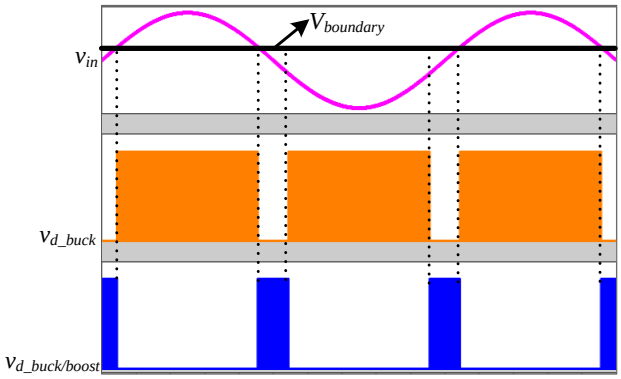

Figure.7. Switches' gate drive signal

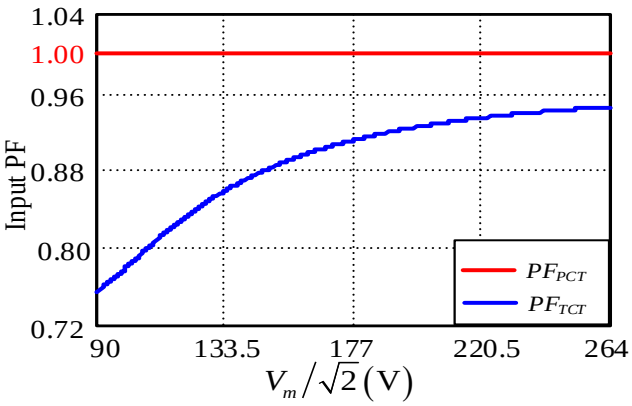

Figure.8. Input PF comparison between TCT and PCT

5. Conclusion

With a constant on-time of a buck-boost converter, the peak & rms values of the inductor current are high due to switching and conduction losses. So, efficiency is low. To achieve maximum efficiency with minimum losses, simple

design and cheap component cost, a control strategy is suggested in this paper. To verify the analysis simulation results are provided.

References

[1] Memon, A.H., Noonari, F.M., Memon, Z., Farooque, A. and Uqaili, M.A., 2020. AC/DC critical conduction mode buck-boost converter with unity power factor.

[2] Yao, K., Ruan, X., Mao, X. and Ye, Z., 2010. Variable-duty-cycle control to achieve high input power factor for DCM boost PFC converter. IEEE Transactions on Industrial Electronics, 58(5), pp.1856-1865.

[3] Y. Fei, R. Xinbo, Y. Yang, and Y. Zhihong, "Interleaved critical current mode boost PFC converter with coupled inductor," IEEE Trans. Power Electron., vol. 26, no. 9, pp. 2404–2413, Sep. 2011.

[4] O. Garcia, J. A. Cobos, R. Prieto, P. Alou, and J. Uceda, "Single phase power factor correction: a survey," IEEE Trans. Power Electron., vol. 18, no. 3, pp. 749-755, May 2003.

[5] Singh, B. N. Singh, A. Chandra, K. Al-Haddad, A. Pandey, and D. P. Kothari, "A review of single-phase improved power quality AC/DC converters," IEEE Trans. Ind. Electron., vol. 50, no.5, pp.962-981, Oct. 2003.

[6] Memon, A. (2020). DCM Boost Converter With High Efficiency. Journal Of Mechanics Of Continua And Mathematical Sciences. spl6. 10.26782/jmcms.spl.6/2020.01.00006.

[7] Memon, A. (2020). Realization Of Unity Power Factor For Ac/Dc Boundary Conduction Mode Flyback Converter With Any Specific Turn's Ratio. Journal Of Mechanics Of Continua And Mathematical Sciences. spl6. 10.26782/jmcms.spl.6/2020.01.00014.

[8] T. Hwang and S. Park, "Seamless boost converter control under the critical boundary condition for a fuel cell power conditioning system," IEEE Trans. Power Electron., vol. 27, no. 8, pp. 3616-3626, Aug. 2012.

[9] F. Chen and D. Maksimović, "Digital control for improved efficiency and reduced harmonic distortion over wide load range in boost PFC rectifiers," IEEE Trans. Power Electron., vol. 25, no. 10, pp. 2683-2692, Oct. 2010

[10] M. Mahdavi and H. Farzanehfard, "Bridgeless SEPIC PFC rectifier with reduced components and conduction losses," IEEE Trans. Ind. Electron., vol. 58, no. 9, pp. 4153-4160, Sep. 2011.

[11] X. Liu, J. Xu, Z. Chen, and N. Wang, "Single-inductor dual-output buck-boost power factor correction converter," IEEE Trans. Ind. Electron., vol. 62, no. 2, pp. 943-952, Feb. 2015

[12] Electromagnetic Compatibility (EMC), Part 3-2: Limits—Limits for harmonic current emissions (Equipment input current ≤16 A per phase), Int. Std. IEC 61000-3-2, 2005.

[13] IEEE recommended practice and requirements for harmonic control in electric power systems, of IEEE Standard 519-2014, Revision of IEEE Standard, 2014.

[14] H. Endo, T. Yamashita, T. Sugiura, "A high-power-factor buck converter," in Proc. IEEE Power Electron. Spec. Conf., Toledo, Spain, 1992, pp. 1071-1076

[15] X. Wu, J. Yang, J. Zhang and M. Xu, "Design considerations of soft-switched buck PFC converter with constant on-time (COT) control," IEEE Trans. Power Electron., vol. 26, no. 11, pp. 3144-3152, Nov. 2011.

[16] X. Wu, J. Yang, J. Zhang and Z. Qian, "Variable on-time (VOT)-controlled critical conduction mode buck PFC converter for high-input AC/DC HB-LED lighting applications," IEEE Trans. Power Electron., vol. 27, no. 11, pp. 4530-4539, Nov. 2012.

[17] Memon, A.H., Yao, K., Chen, Q., Guo, J. and Hu, W., 2016. Variable-on-time control to achieve high input power factor for a CRM-integrated buck–flyback PFC converter. IEEE Transactions on Power Electronics, 32(7), pp.5312-5322.

[18] Memon, A.H. and Yao, K., 2018. UPC strategy and implementation for buck–buck/boost PF correction converter. IET Power Electronics, 11(5), pp.884-894.

[19] Memon, A.H., Baloach, M.H., Sahito, A.A., Soomro, A.M. and Memon, Z.A., 2018. Achieving High Input PF for CRM Buck-Buck/Boost PFC Converter. IEEE Access, 6, pp.79082-79093.

[20] Memon, A.H., Memon, M.A., Memon, Z.A. and Hashmani, A.A., 2019. Critical Conduction Mode Buck-Buck/Boost Converter with High Efficiency.

[21] Memon, A.H., Memon, Z.A., Shaikh, N.N., Sahito, A.A. and Hashmani, A.A., 2019. Boundary conduction mode modified buck converter with low input current total harmonic distortion. Indian Journal of Science and Technology, 12, p.17.

[22] Memon, A.H., Nizamani, M.O., Memon, A.A., Memon, Z.A. and Soomro, A.M., 2019. Achieving High Input Power Factor for DCM Buck PFC Converter by Variable Duty-Cycle Control.

[23] Memon, A.H., Pathan, A.A., Kumar, M. and Sahito, A., A J., & Memon, ZA (2019). Integrated buck-flyback converter with simple structure and unity power factor. Indian Journal of Science and Technology, 12, p.17.

[24] Memon, A.H., Shaikh, N.N., Kumar, M. and Memon, Z.A., 2019. Buck-buck/boost converter with high input power factor and non-floating output voltage. International Journal of Computer Science and Network Security, 19(4), pp.299-304.

[25] Liu, X., Wan, Y., He, M., Zhou, Q. and Meng, X., 2020. Buck-Type Single-Switch Integrated PFC Converter With Low Total Harmonic Distortion. IEEE Transactions on Industrial Electronics.

[26] Memon, A.H., Ali, R. and Memon, Z.A., 2021. Discontinuous conduction mode Buck converter with high efficiency. 3C Tecnol, 10, pp.35-51.

[27] Memon, A.H., Ali, M., Memon, Z.A. and Hashmani, A.A., 2021. Crm Buck Converter With High Input Power Factor. 3C Tecnologia, 10.